

# Towards Accurate Ab Initio QM/MM Calculations of Free-Energy Profiles of Enzymatic Reactions

Edina Rosta, Marco Klähn, and Arieh Warshel\*

Department of Chemistry, University of Southern California, 3620 South McClintock Avenue, Los Angeles, California, 90089-1062

Received: December 6, 2005

Reliable studies of enzymatic reactions by combined quantum mechanical/molecular mechanics (QM/MM) approaches, with an ab initio description of the quantum region, presents a major challenge to computational chemists. The main problem is the need for a large amount of computer time to evaluate the QM energy, which in turn makes it extremely challenging to perform proper configurational sampling. This work presents major progress toward the evaluation of ab initio QM/MM free-energy surfaces and activation free energies of reactions in enzymes and in solutions. This is done by exploiting our previous idea of using the empirical valence bond (EVB) method as a reference potential and then using the linear response approximation (LRA) approach to evaluate the free energies of transfer from the EVB to the QM/MM surfaces in the reactant and product state. However, the new crucial step involves the use of a constraint at the transition state that fixes the system at a given value of the reaction coordinate and allows us to use the LRA at the transition state. The advance offered by the present approach is particularly significant because it evaluates the free energy associated with both the substrate and the solvent motions. This evaluation appeared to be a relatively simple task once one uses a classical reference potential. The main problem has been using the reference potential for the evaluation of the free-energy contributions associated with the solute motions where the difference between the reference EVB potential and the QM/MM potential can be large. The present refinement finally allows us to overcome the problems with the solute fluctuations and therefore to obtain, for the first time, a free-energy barrier that reflects the solute entropy properly. Thus, we present a way to evaluate the complete QM/MM activation free energy with an equal footing treatment of the solute and the solvent. This provides a general consistent and effective strategy for evaluating the QM/MM activation free energies in proteins and in solution. Our advance allows one to explore consistently various mechanistic and catalytic proposals while using ab initio (ai) QM/MM approaches.

## I. Introduction

QM/MM approaches have provided a general scheme for studies of chemical processes in proteins (e.g., refs 1–11). A significant progress has been made with calibrated semiempirical QM/MM approaches (e.g., refs 2, 7, 10, 11) that include careful evaluations of the relevant activation free energies by free-energy perturbation approaches that date back to the 1980s (e.g., ref 12). However, the current challenge is to move to an ab initio representation with a QM/MM treatment because such QM(ai) representations have been shown to provide “chemical accuracy” in studies of gas-phase reactions of small molecules. Unfortunately, it is at present impractical to evaluate the potential of mean force (PMF) for enzymatic reactions by QM(ai)/MM approaches because of the requirement of a very extensive sampling and thus extremely expensive repeated evaluation of the QM energies.

Recent realization of the importance of the proper sampling of QM(ai)/MM sampling led to several advances.<sup>13–23</sup> The main direction of the recent advance has been based on different adaptations<sup>17–22</sup> of our idea<sup>13,14</sup> of using a classical potential as a reference for the QM/MM calculations. However, a key point that has been perhaps overlooked in some of the recent studies (e.g., refs 17 and 18) is the challenge of obtaining the free energy of the solute and not just the surrounding solvent. That is,

simulations with a fixed solute miss the crucial entropic contribution of the solute configuration and this contribution cannot be estimated by the harmonic approximation, at least when one deals with activation free energies of reactions in condensed phases (see the discussion in ref 24). Furthermore, calculations that estimate the QM/MM solute path along a fixed-energy minimized path may reflect artificial minima in the complex landscape of the enzyme active site.<sup>25</sup> Now, as demonstrated in our early works, it is rather simple to obtain converging results using a classical reference potential once the solute is fixed.<sup>26</sup> The problems start when the solute is allowed to fluctuate. In this case, even with the EVB as a reference potential, there can be a significant difference between the QM/MM potential and the reference potential. In fact, overlooking this problem leads to misunderstandings and the assumption that our early works have been less effective than their recent adaptations.<sup>18</sup>

A significant part of our effort in the past few years has been focused on the challenge of obtaining converging results when the solute is allowed to fluctuate. This led to a development of a linear response approximation treatment that allowed us to obtain a reasonable convergence even in the challenging case of the auto dissociation of water in water.<sup>14</sup> However, we were less successful in obtaining the activation barrier because the LRA formulation was not derived for this case. Thus, we were unable to provide a general prescription for evaluating QM(ai)/MM activation free energies.

\* Corresponding author. E-mail: warshel@usc.edu.

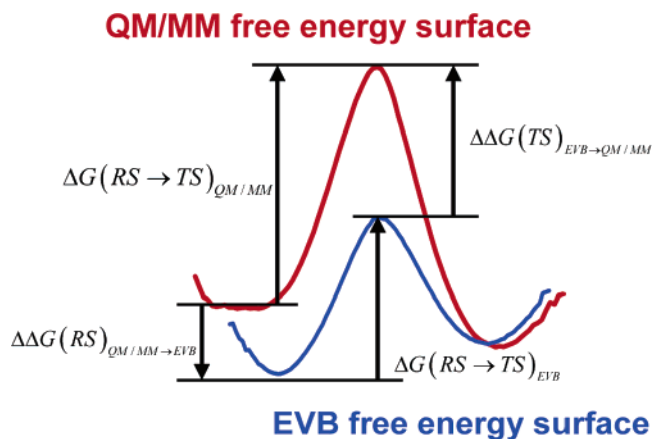


**Figure 1.** Thermodynamic cycle used to evaluate the QM/MM activation barrier.

In the present work, we report a modification of our LRA treatment that finally allows us to obtain converging QM(ai)/MM activation free energies while considering the effect of the substrate motion. This presents, in our view, very significant progress in QM/MM simulations, where it is finally possible to evaluate the activation free energies of enzymatic reactions by ab initio QM/MM approaches and doing this without enormous computational effort.

Our approach is demonstrated in a study of the  $S_N2$  reaction of haloalkane dehalogenase and its corresponding reference solution reaction. It is shown that we can now obtain the catalytic effect of enzymatic reactions by QM(ai)/MM approaches.

## II. Methods and Systems

Our approach is based on the thermodynamic cycle of Figure 1. In this cycle we have a reference free-energy surface,  $\Delta g_{\text{EVB}}$ , which is used to evaluate the QM/MM activation free energy.

To progress in a rigorous way, we start by defining the configurational partition function of the system

$$Q_\alpha = \int \int e^{-\Delta E_\alpha(x,\tau)\beta} dx d\tau = c_\tau \int_{-\infty}^{\infty} e^{-\Delta g_\alpha(x)\beta} dx \quad (1)$$

where  $E_\alpha$  is the given potential surface ( $\alpha$  is taken as  $a$  or  $b$  for the EVB or QM/MM surfaces, respectively),  $x$  is the reaction coordinate, and  $\tau$  are all of the coordinates perpendicular to the reaction coordinate,  $\Delta g_\alpha$  is the resulting free-energy profile along the reaction coordinate, and  $c_\tau$  is a constant.

Next, we define the partition function and free energy of the reactant (RS) (or product (PS)) state by

$$Q_\alpha(\text{RS}) = c_\tau \int_{-\infty}^{x^\ddagger} e^{-\Delta g_\alpha(x)\beta} dx = c_\tau \int_{-\infty}^{x^\ddagger} \frac{q_\alpha(x)}{c_x} dx = \frac{c_\tau}{c_x} c_x e^{-\Delta G_\alpha(\text{RS})\beta} \quad (2)$$

This expression can provide the free energy of the reaction by

$$\Delta G_\alpha(\text{RS} \rightarrow \text{PS}) = \Delta G_\alpha(\text{PS}) - \Delta G_\alpha(\text{RS}) \quad (3)$$

We can also use the  $\Delta g(x)$  function to evaluate the rate constant in our multidimensional surface by (for details see refs 27 and 28)

$$k_\alpha = \kappa \left( \frac{1}{2} \langle |\dot{x}| \rangle_{\text{TS}} / \Delta x^\ddagger \right) \exp\{-\Delta g_\alpha(x^\ddagger)\beta\} \left( \Delta x^\ddagger / \int_{-\infty}^{x^\ddagger} \exp\{-\Delta g_\alpha(x)\beta\} dx \right) = \kappa \left( \frac{1}{2} \langle |\dot{x}| \rangle_{\text{TS}} / \Delta x^\ddagger \right) \exp\{-\Delta G_\alpha^\ddagger\beta\} \quad (4)$$

where  $\kappa$  is the transmission factor,  $\dot{x}$  is the velocity along the reaction coordinate, and  $\Delta x^\ddagger$  is the width of transition state (TS) region.  $\Delta G_\alpha^\ddagger$  is defined by eq 4 and can be expressed as

$$\Delta G_\alpha^\ddagger = \Delta g_\alpha(x^\ddagger) - \Delta g_\alpha(x_{\text{RS}}^0) + \beta^{-1} \ln \left[ \frac{1}{\Delta x^\ddagger} \int_{-\infty}^{x^\ddagger} \exp\{-(\Delta g_\alpha(x) - \Delta g_\alpha(x_{\text{RS}}^0))\beta\} dx \right] \quad (5)$$

where  $x_{\text{RS}}^0$  is the lowest point at the RS. The correction by the last term in the equation provides a convenient way of incorporating the entropic effects of the ground state into the transition-state-theory rate constant.<sup>27</sup> This correction is in fact the origin of our  $\Delta g_w^\ddagger - \Delta g_{\text{cage}}^\ddagger$  term (see, e.g., refs 24 and 29).

To evaluate the  $\Delta G_{\text{QM/MM}}(\text{RS})$  and  $\Delta g_{\text{QM/MM}}(x_{\text{QM}}^\ddagger)$  terms of eq 5, we exploit the availability of the EVB reference surface and write

$$\Delta G_b(\text{RS}) = \Delta G_a(\text{RS}) + \Delta \Delta G_{a \rightarrow b}(\text{RS}) \quad (6)$$

and

$$\Delta g_b(x_b^\ddagger) = \Delta g_a(x_b^\ddagger) + \Delta \Delta g_{a \rightarrow b}(x_b^\ddagger) \quad (7)$$

The  $\Delta \Delta G(\text{RS})$  term is evaluated by the LRA end point approach of ref 14 using

$$\Delta \Delta G_{a \rightarrow b}(\text{RS}) = -\beta^{-1} \ln(Q_b(\text{RS})/Q_a(\text{RS})) = -\beta^{-1} \ln[\langle \exp\{-(E_b - E_a)\beta\} \rangle_a] \approx \frac{1}{2} (\langle E_b - E_a \rangle_a + \langle E_b - E_a \rangle_b) \quad (8)$$

where we approximated the free-energy perturbation treatment by the LRA expression. It is useful to note that the exponential average  $\langle \exp\{-(E_b - E_a)\beta\} \rangle_a$  in eq 8 is just a formal expression that is usually evaluated by a free-energy perturbation treatment.

The  $\Delta \Delta g(x^\ddagger)$  value is evaluated by the same LRA approach, but now considering the partial partition function at  $x^\ddagger$ . This gives

$$\Delta \Delta g_{a \rightarrow b}(x_b^\ddagger) = -\beta^{-1} \ln(q_b(x_b^\ddagger)/q_a(x_b^\ddagger)) = -\beta^{-1} \ln[\langle \exp\{-(E_b(x_b^\ddagger) - E_a(x_b^\ddagger))\beta\} \rangle_a] \approx \frac{1}{2} (\langle E_b(x_b^\ddagger) - E_a(x_b^\ddagger) \rangle_a + \langle E_b(x_b^\ddagger) - E_a(x_b^\ddagger) \rangle_b) \quad (9)$$

Up to this point in the derivation the main advance is the idea of fixing the system at  $x^\ddagger$ . However, even with this seemingly simple idea we have a significant problem because the transition state for the EVB ( $a$ ) and QM/MM ( $b$ ) free-energy surfaces can be different. To resolve this problem, we start by modifying eq 9 by using

$$\Delta g_b(x_b^\ddagger) = \Delta g_a(x_a^\ddagger) + \Delta \Delta g_{a \rightarrow b}(x_a^\ddagger) + \Delta \Delta g_b(x_a^\ddagger \rightarrow x_b^\ddagger) \quad (10)$$

The last term can be evaluated by calculating the potential of mean force (PMF) for moving on the QM/MM surface from  $x_{\text{EVB}}^\ddagger$  to  $x_{\text{QM/MM}}^\ddagger$ . The PMF calculations can be performed by defining two sets of constraints (one for  $x_{\text{QM/MM}}^\ddagger$  and the other for  $x_{\text{EVB}}^\ddagger$ ) and pulling the system from one constraint to another

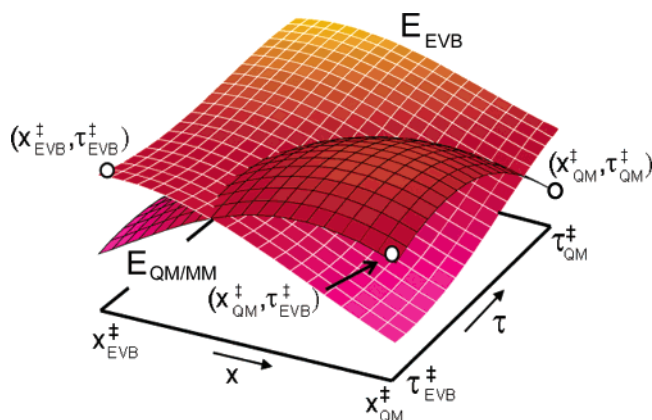


**Figure 2.** Schematic description of the intersection of  $E_{\text{EVB}}$  and  $E_{\text{QM/MM}}$  at the TS region. The figure can be used as a qualitative illustration (see the text) for the validity of the LRA treatment of eqs 9 and 12.

on the QM/MM surface. Furthermore, we are able to use the LRA formulation and derive an expression that evaluates the last two terms of eq 10 in one step, in which case the reaction coordinates,  $x_{\text{EVB}}$  and  $x_{\text{QM/MM}}$ , can also be different. With this formulation, we write

$$\Delta g_b(x_b^\ddagger) = \Delta g_a(x_a^\ddagger) + \Delta \Delta g_{a \rightarrow b}(x_a^\ddagger \rightarrow x_b^\ddagger) \quad (11)$$

This can be done by including the coordinate  $x^\ddagger$  in the LRA treatment and writing

$$\Delta g_b(x_b^\ddagger) - \Delta g_a(x_a^\ddagger) = \Delta \Delta g_{a \rightarrow b}(x_a^\ddagger \rightarrow x_b^\ddagger) \cong \frac{1}{2} [\langle E_b(x_a^\ddagger) - E_a(x_a^\ddagger) \rangle_a + \langle E_b(x_b^\ddagger) - E_a(x_b^\ddagger) \rangle_b] \quad (12)$$

This new expression will be used in the present work in the evaluation of  $\Delta g_{\text{QM/MM}}(x_{\text{QM/MM}}^\ddagger)$ .

To clarify the main elements of our new LRA concept, we illustrate in Figure 2 a typical behavior of  $E_{\text{EVB}}$  and  $E_{\text{QM/MM}}$  at the transition state (TS) region. The figure considers these two surfaces in the simplifying case when the reaction coordinate,  $x$ , is similar for both surfaces (this is not a formal requirement in our treatment) and the same set of coordinates,  $\tau$ , which span the space perpendicular to  $x$ . Our task is to find the free-energy change associated with the move from  $E_{\text{EVB}}(x_{\text{EVB}}^\ddagger, \tau_{\text{EVB}}^\ddagger)$  to  $E_{\text{QM/MM}}(x_{\text{QM/MM}}^\ddagger, \tau_{\text{QM/MM}}^\ddagger)$ . Now, the motion along the  $\tau$  axis can be described clearly by the LRA approximation because it corresponds to two parabolas leading to eq 9. Similarly, the motion along the  $x$  axis can be described by the LRA because it corresponds to the intersection of two inverted parabolas. The overall application of eq 12 corresponds to the motion from  $(x_{\text{EVB}}^\ddagger, \tau_{\text{EVB}}^\ddagger)$  to  $(x_{\text{QM/MM}}^\ddagger, \tau_{\text{QM/MM}}^\ddagger)$  and is also described by the LRA approach because it corresponds to transitions between two surfaces that can be approximated by  $E_{\text{EVB}}(\delta Q_i) \approx \sum_i \lambda_i (\delta Q_i)^2$  and  $E_{\text{QM/MM}}(\delta Q_i) \approx \sum_i \lambda'_i (\delta Q_i + \Delta)^2$ , respectively, where only one of the  $\lambda$  coefficients is negative in each case ( $\delta Q_i$  are the displacements from the TS after principal axis transformation).

It is useful to point out at this point that the calculations of  $\Delta \Delta g_{\text{EVB-QM/MM}}(x_{\text{EVB}}^\ddagger \rightarrow x_{\text{QM/MM}}^\ddagger)$  allow the solvent to relax at the TS of the solute coordinate. Such an approach misses the so-called nonequilibrium solvation (NES) effect (see the discussion in ref 30). Fortunately, the  $\Delta g(x_{\text{EVB}}^\ddagger)_{\text{EVB}}$  value is evaluated by the EVB mapping procedure<sup>27</sup> that captures the NES free energy. Assuming that the NES contribution is similar in the

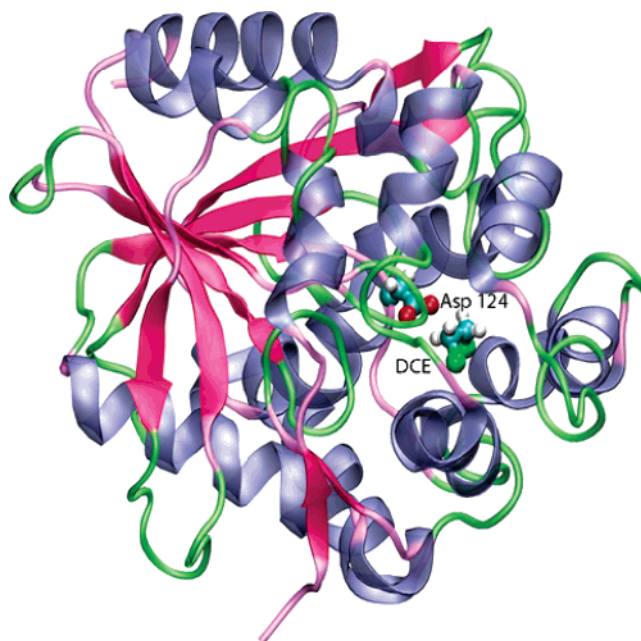


**Figure 3.** Overall structure of DhIA with the active site Asp124 and a bound DCE.

QM/MM and EVB surfaces, we can treat  $\Delta g(x_{\text{QM/MM}}^\ddagger)_{\text{QM/MM}}$  as the correct activation free energy that contains the NES effects.

To validate our approach, we took the first step in the reaction of haloalkane dehalogenase (DhIA) as a benchmark (see the references in ref 31) using the crystal structure of the enzyme<sup>32</sup> as a starting point (2DHD). This system catalyzes the cleavage of the halogen from dichloroethane (DCE) and similar alkyl-halides by an  $S_N2$  nucleophilic attack of the oxygen of Asp 124 on the carbon of the DCE (see Figure 3). In the second step of the enzymatic reaction, the formed ester is hydrolyzed by a water molecule resulting in an alcohol as the final product. These reaction steps are illustrated in Figure 4. The  $S_N2$  step of the reaction of DhIA has been subject to many recent theoretical and experimental studies<sup>29,31,33–47</sup> and, of course, the  $S_N2$  reaction has also been a central subject in physical organic chemistry (e.g., ref 48). The EVB potential surface has been described in detail in previous works.<sup>31</sup> The QM(ai)/MM surface was evaluated as described in detail in 25. Our treatment used a standard link atom technique rather than the more reliable hybrid orbital type treatments (e.g., refs 1 and 49) because we found it very convenient to link our MM program MOLARIS<sup>50</sup> to standard QM programs (in this case GAUSSIAN 98<sup>51</sup>) through an automated external script. The QM system consisted of the dichloroethane and the formate group, treating a total of 12 atoms quantum mechanically. The hydrogen atom of the formate ion is treated as a link atom to the carbons of the Asp 124 residue and the methyl group for the reactions in the protein and in the reference solution reaction, respectively. The quantum system was treated by the B3LYP/DFT method with the 6-31G\* basis set.

The specific EVB parameters used in this work constitute a small modification of the parameters that were used in ref 31. The EVB-MD simulations were performed using the MOLARIS program with a simulation sphere of 22 Å described by the ENZYME force field and subject to the surface constraint all atom solvent (SCAAS)<sup>12</sup> spherical boundary conditions and the local reaction field (LRF) long-range treatment.<sup>12</sup> The EVB free-energy profile of the reacting systems (water and protein) was evaluated by performing the EVB FEP/umbrella sampling (US)



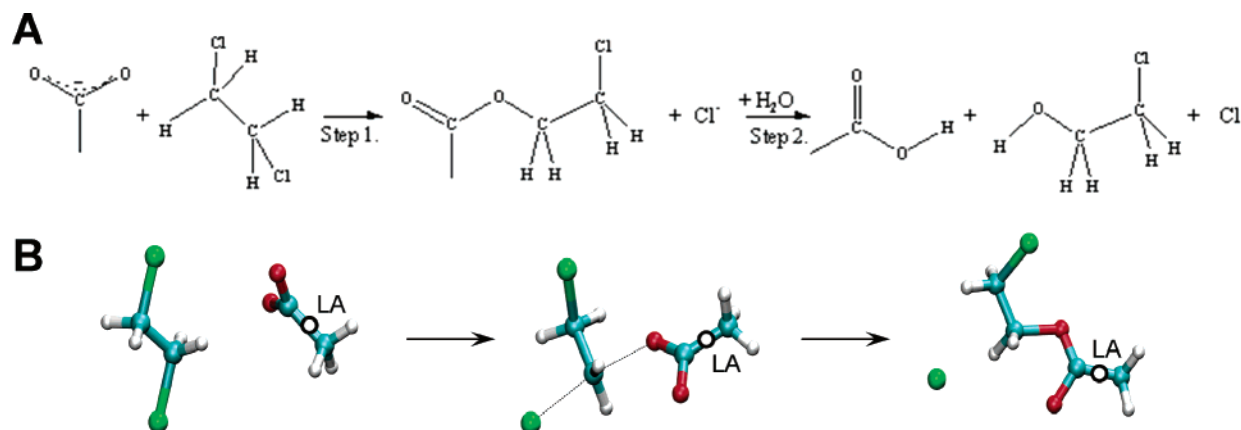


**Figure 4.** Schematic description of the reaction steps in DhIA (4A) and a stick diagram describing the S<sub>N</sub>2 step for the reaction in water with an illustration of the link atom (4B).

**TABLE 1: EVB Energetics of the S<sub>N</sub>2 Reaction in Water and in Haloalkane Dehalogenase for Simulations with Five Different Initial Conditions<sup>a</sup>**

EVB mapping	water		protein	
	$\Delta\Delta G(\text{RS} \rightarrow \text{TS})$	$\Delta\Delta G(\text{RS} \rightarrow \text{PS})$	$\Delta\Delta G(\text{RS} \rightarrow \text{TS})$	$\Delta\Delta G(\text{RS} \rightarrow \text{PS})$
sim 1	26.97	-1.11	19.82	4.47
sim 2	28.32	-6.19	19.53	3.67
sim 3	29.48	-5.43	19.98	4.52
sim 4	28.86	-5.27	20.37	5.87
sim 5	28.09	-0.47	19.39	3.75
average	28.34	-3.69	19.82	4.46

<sup>a</sup> The energies are given in kcal/mol.

procedure with 31 windows of 10-ps length each and a time step of 1 fs. The simulations were performed at 300 K.

### III. Results and Discussion

As stated in the previous section, we took the first step in the reaction of DhIA as our benchmark system. The calculations started with the evaluation of the EVB free-energy surface for the reaction in DhIA and in the reference solution system. The final free-energy profiles were then obtained by averaging the results of five mapping calculations from different initial conditions, each obtained after 100 ps relaxation at the reactant state. The simulation system for the reference reaction in water is depicted in Figure 5. The results of the simulations are summarized in Table 1. The corresponding EVB surfaces are described in Figure 6.

In the next step we perform the LRA calculations of the  $\langle E_b - E_a \rangle$  terms of eq 8 (where  $a$  and  $b$  designate the EVB and QM/MM surfaces, respectively). The fluctuations involved in these simulations are illustrated in Figure 7, the corresponding distributions are shown in Figure 8, and the resulting averages are summarized in Table 2. These results were then used to convert the EVB reaction energy to the QM/MM free energy using eq 6. This treatment gave a  $\Delta G(\text{RS} \rightarrow \text{PS})_{\text{QM/MM}}$  value of -10.42 and -2.25 kcal/mol for the reaction in the protein and water, respectively.

Finally, we turn to the QM/MM TS for the reaction in water and in the protein active site (the structure of the TS in the protein active site is described in Figure 9). Although our approach allows us to evaluate the ab initio barrier by using the EVB barrier, we face the challenge of finding configurations that constitute  $x_{\text{QM/MM}}^\ddagger$  without actually calculating the entire  $\Delta G_{\text{QM/MM}}(x)$ . Our way to overcome the challenge is to exploit the fact that in many cases (e.g., S<sub>N</sub>2 and related reactions)  $x_{\text{p}}^\ddagger \approx x_{\text{w}}^\ddagger \approx x_{\text{gas}}^\ddagger$  (see, e.g., ref 52). Taking  $x_{\text{EVB}}^\ddagger$  to be our

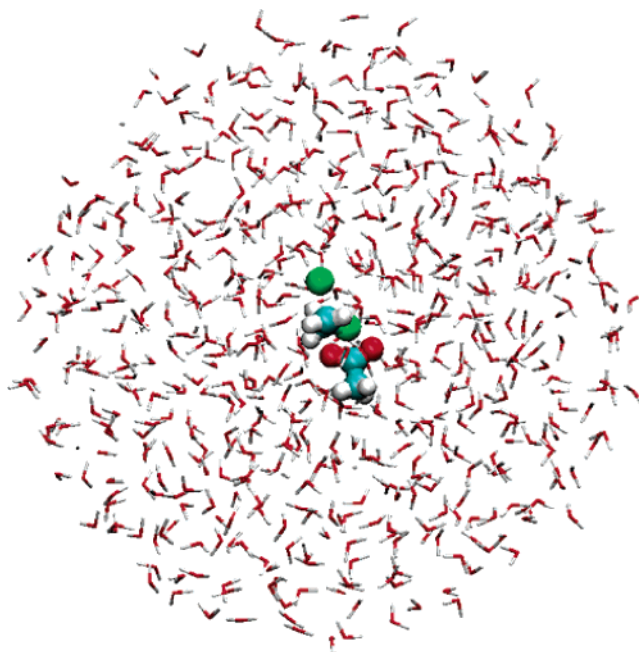


**Figure 5.** SCAAS simulation system for the reference reaction in water.

approximation for the TS of both the QM and the EVB potentials, we obtained the results that are illustrated in Figure 10 and summarized in the first two columns of Tables 3 and 4, respectively, for the solution and protein reactions. Now, if our assessment that the TSs are similar for the QM/MM and EVB potentials is correct, there is no need to evaluate the last two terms in eq 10. With this in mind, we obtained a first rough estimate of the effect of moving to  $x_{\text{QM/MM}}^\ddagger$  by evaluating the average force along the reaction coordinate at  $x_{\text{EVB}}^\ddagger$  for trajectories on the EVB and on the QM/MM surface. In both cases, we found the average forces to be similar indicating that the

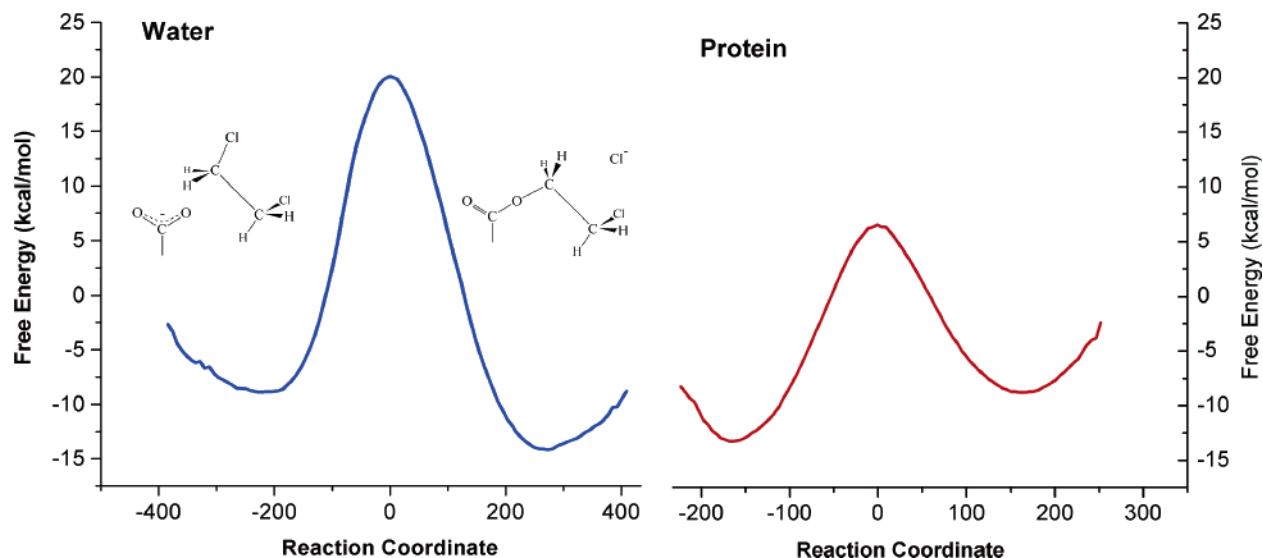


**Figure 6.** EVB free-energy profile of the  $S_N2$  reaction in water and in the haloalkane dehalogenase enzyme. The profiles were obtained using FEP/QM for the EVB ground-state energy.

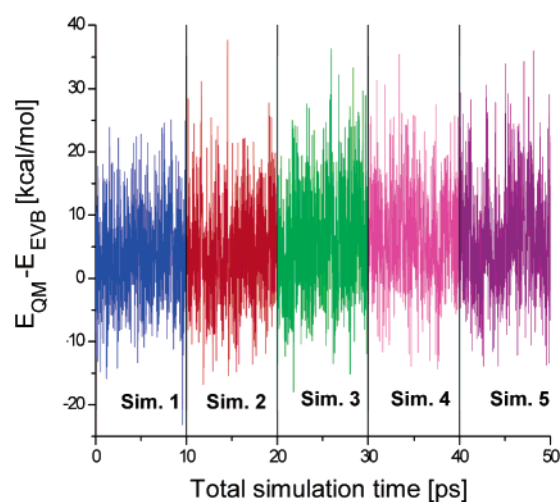


**Figure 7.** Fluctuations of  $E_{QM/MM} - E_{EVB}$  for runs on the transition state of the EVB surface at  $x_{EVB}^{\ddagger}$ . The figure depicts the results of 5 runs, each of 10 ps.

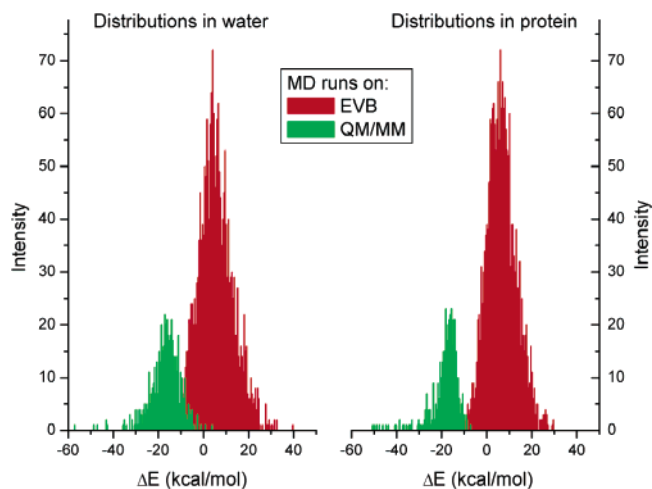


**Figure 8.** Distributions of  $E_{QM/MM} - E_{EVB}$  for trajectories on the potential energy surfaces of the EVB and the QM/MM reactant states.

above approximation is reasonable in the present case. The second and more rigorous estimate of the QM/MM estimate involves the use of eqs 11 and 12 for a direct evaluation of the

**TABLE 2: LRA Estimate of the Free Energy of Transfer from the EVB to the QM/MM Surface in the RS and PS for the Reaction of Dh1A<sup>a</sup>**

	water	protein
$\langle E_{QM/MM} - E_{EVB} \rangle_{EVB(RS)}$	5.49	6.81
$\langle E_{QM/MM} - E_{EVB} \rangle_{EVB(PS)}$	5.30	2.36
$\langle E_{QM/MM} - E_{EVB} \rangle_{QM/MM(RS)}$	-16.60	-19.27
$\langle E_{QM/MM} - E_{EVB} \rangle_{QM/MM(PS)}$	-29.88	-28.25
$\Delta\Delta G(PS)_{EVB \rightarrow QM/MM}$	-6.73	-6.71

<sup>a</sup> Energies are given in kcal/mol.  $\Delta\Delta G(PS)$  is given relative to  $\Delta\Delta G(RS)$  and the results reflect the average of two simulation runs.

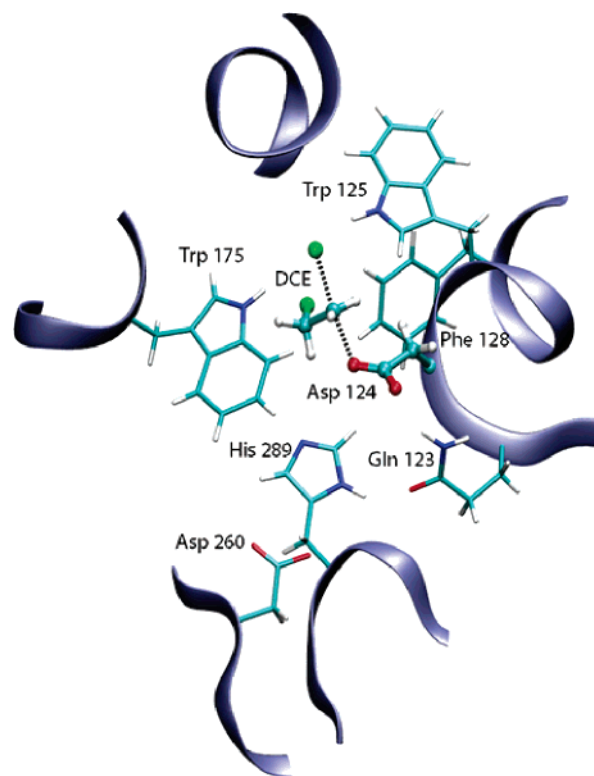


**Figure 9.** TS of the  $S_N2$  reaction step in the active site of Dh1A.

QM/MM free energy at the gas-phase estimate of  $x_{QM/MM}^{\ddagger}$ . This gave  $\Delta G_{QM/MM,enz}^{\ddagger} = 18.6$  kcal/mol and  $\Delta G_{QM/MM,wat}^{\ddagger} = 27.6$  kcal/mol. The corresponding calculated catalytic effect is  $\Delta\Delta G^{\ddagger}$

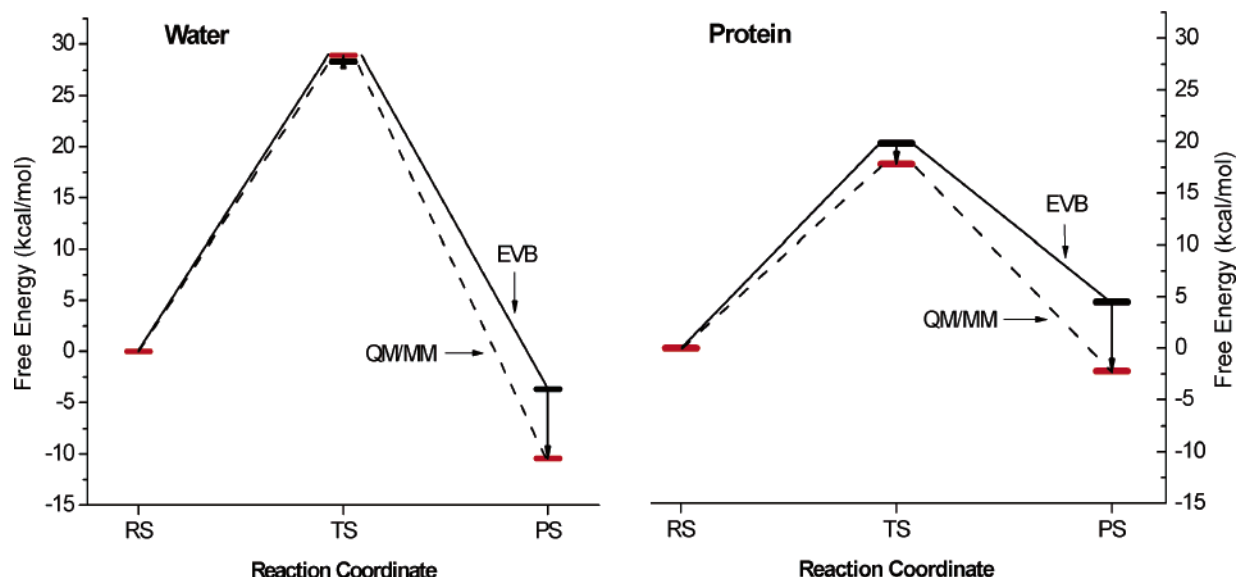


Figure 10. Obtaining the QM/MM activation free energy by moving from the EVB to the QM/MM surfaces.

TABLE 3: Results of the LRA Simulation for the Transition State of the Solution Reaction and the Overall QM/MM Activation Barrier<sup>a</sup>

water TS simulations	$\langle E_b(x_a^\ddagger) - E_a(x_a^\ddagger) \rangle_b$	$\langle E_b(x_a^\ddagger) - E_a(x_a^\ddagger) \rangle_a$	$\langle E_b(x_b^\ddagger) - E_a(x_b^\ddagger) \rangle_b$
sim 1	-15.70	3.52	-17.64
sim 2	-18.24	4.01	-17.83
sim 3	-16.98	5.77	-18.33
sim 4	-11.58	6.42	-17.32
sim 5	-13.34	6.17	-17.43
average	-15.17	5.18	-17.71
average with RS as a reference	1.43	-0.31	-1.11
overall $\Delta G^\ddagger$	$\Delta\Delta g_{a \rightarrow b}(x_a^\ddagger) =$ $(1.43 + -0.31)/2 = 0.56$ $28.34 + 0.56 = 28.90$ (obs: 27.0)		$\Delta\Delta g_{a \rightarrow b}(x_a^\ddagger \rightarrow x_b^\ddagger) =$ $(-0.31 + -1.11)/2 = -0.71$ $28.34 - 0.71 = 27.63$ (obs: 27.0)

<sup>a</sup> The energies are given in kcal/mol. The subscripts *a* and *b* designate, respectively, the EVB and QM/MM potential surfaces. The lower part of the table provides two estimates for  $\Delta G^\ddagger$ ; the first involves the use of the first two terms of eq 10 assuming that  $x_{\text{EVB}}^\ddagger \approx x_{\text{QM/MM}}^\ddagger$ . The second one involves the use of eqs 11 and 12, while taking  $x_{\text{QM/MM}}^\ddagger$  from the corresponding gas-phase estimates. The observed activation barrier is taken from the estimate of ref 31.

TABLE 4: Results of LRA Simulations at the Transition State of the Enzyme Reaction and the Overall QM/MM Activation Barrier<sup>a</sup>

protein TS simulations	$\langle E_b(x_a^\ddagger) - E_a(x_a^\ddagger) \rangle_b$	$\langle E_b(x_a^\ddagger) - E_a(x_a^\ddagger) \rangle_a$	$\langle E_b(x_b^\ddagger) - E_a(x_b^\ddagger) \rangle_b$
sim 1	-16.51	-2.18	-15.09
sim 2	-16.59	-0.85	-14.00
sim 3	-17.17	-2.74	-15.08
sim 4	-16.45	0.43	-15.19
sim 5	-16.14	5.97	-15.10
average	-16.61	0.13	-14.89
average with RS as a reference	2.70	-6.68	4.38
overall $\Delta G^\ddagger$	$\Delta\Delta g_{a \rightarrow b}(x_a^\ddagger) =$ $(2.70 + -6.68)/2 = -1.99$ $19.82 - 1.99 = 17.83$ (obs: 15.3 <sup>a</sup> )		$\Delta\Delta g_{a \rightarrow b}(x_a^\ddagger \rightarrow x_b^\ddagger) =$ $(-6.68 + 4.38)/2 = -1.15$ $19.82 - 1.15 = 18.67$ (obs: 15.3 <sup>a</sup> )

<sup>a</sup> The energies are given in kcal/mol. The subscripts *a* and *b* designate, respectively, the EVB and QM/MM potential surfaces. The lower part of the table provides two estimates for  $\Delta G^\ddagger$ ; the first involves the use of the first two terms of eq 10 assuming that  $x_{\text{EVB}}^\ddagger \approx x_{\text{QM/MM}}^\ddagger$ . The second one involves the use of eqs 11 and 12, while taking  $x_{\text{QM/MM}}^\ddagger$  from the corresponding gas-phase estimates. The observed activation barrier is taken from the estimate of ref 31.

$= \Delta G_{\text{wat}}^\ddagger - \Delta G_{\text{enz}}^\ddagger \approx 9$  kcal/mol, whereas the estimate based on the first two terms of eq 10 gives  $\Delta\Delta G_{\text{QM/MM}}^\ddagger \approx 11$  kcal/mol.

Thus, our results are in good agreement with the corresponding observed value ( $\Delta\Delta G_{\text{obs}}^\ddagger = 11.7$  kcal/mol).

**TABLE 5: Gas-Phase Ab Initio Activation Energies for the Attack of a Carboxylate on DCE<sup>a</sup>**

	B3LYP 6-31G*	B3LYP 6-611++G**	MP2 6-31G*	MP2 6-311++G**	G2 <sup>45</sup>
formate + DCE <sup>b</sup>	17.04 (+1.86)	17.22 (+2.43)	24.70 (−1.65)	25.36 (−2.26)	
acetate + DCE	18.13	18.35	25.88	26.18	21.3

<sup>a</sup> The energies are given in kcal/mol. <sup>b</sup> The difference between the solvation free energies of the transition state and the reactant state are given in parentheses. These solvation free energies were evaluated using the Langevin dipoles model.<sup>53</sup>

The present study focuses on the evaluation of the free energy of a given ab initio QM/MM approach without addressing the reliability of the specific QM/MM potential surface. Because we used here the DFT B3LYP method with a 6-31G\* basis set, it is interesting to ask how accurate the results of this method are assuming that we obtain its correct free-energy surface. To explore this issue, we examine the gas-phase ab initio activation free energies of the S<sub>N</sub>2 reaction with formate and acetate as the nucleophiles and with different ab initio models (see Table 5). We found that using larger basis sets including diffuse functions does not change the results significantly, so the choice of 6-31G\* is very reasonable. The DFT/B3LYP method seems to underestimate the transition state barrier by about 8 kcal/mol in the gas phase for the formate system, relative to the MP2/6-311G\*\* results. However, the QM/MM calculations correspond to solution calculations and the difference between the B3LYP/6-31G\* and MP2/6-311G\*\* calculations of formate in a Langevin dipoles (LD) solvent model<sup>53</sup> was found to be about 4 kcal/mol. Furthermore, the gas-phase estimate obtained by CCSD(T)/6-31G\* is only about 23 kcal/mol for the formate system and the G2 results for acetate are only 21.3 kcal/mol. Thus, we estimate that the error associated with the quantum method used and with the use of formate instead of acetate is about 2–3 kcal/mol. We do not expect that a smaller error range can be obtained without addressing such issues as the effect of charge transfer to the solvent and the effect of using polarizable force field (that was not used in this study). With this in mind we believe that it is still important to calibrate or at least to validate the QM/MM results using experimental information about the reference solution reaction. However, the difference between the barrier in the enzyme and in the reference solution reaction should be sufficiently reliable to let one reach clear conclusions about the catalytic effect of the enzyme.

#### IV. Concluding Remarks

The evaluation of the free-energy changes in proteins by classical force fields usually requires a very extensive averaging over the configurational space of the protein. Thus, it is quite likely that the same requirement will hold for QM/MM calculations. This means that simple minimization approaches of the type used in gas-phase QM calculations might not be effective in evaluations of activation energies of chemical reactions in proteins (e.g., see ref 25). Unfortunately, evaluating the activation free energies for QM(ai)/MM surfaces is extremely challenging because of the need of extensive evaluation of the QM(ai) energies.

Here we present a major refinement of our previous treatments<sup>14</sup> that allows one to evaluate the QM(ai)/MM activation free energies of reactions in condensed phases. Our treatment uses, as before, the EVB as a reference potential and then uses the LRA approach to evaluate the free energies of transfer from the EVB to the QM/MM surfaces in the reactant and product state. However, at the transition state we constraint the system to be at a fixed value of the reaction coordinate, using the EVB and QM/MM partial partition functions (the  $q$ 's of eqs 2 and 9) to evaluate the QM/MM free energy at the transition state.

The new version allows us to evaluate the QM(ai)/MM activation free energies for reactions in proteins and solutions in an effective and economical way. This advance is particularly significant because it evaluates the free energy associated with both the substrate and the solvent motions. The evaluation of the free-energy associate with the solvent (or protein) configurational space has been found (e.g., ref 26) to be a relatively simple task when one uses a classical reference potential. The main problem appeared to be associated with the use of the reference potential in evaluation of the free-energy contributions associated with the solute motions, where the difference between the reference EVB potential and the QM/MM potential can be large. The present refinement finally allows us to overcome the problems with the solute fluctuations and thus presents a general way for evaluating QM(ai)/MM activation free energies for reactions in proteins and solutions.

It might be useful to estimate at this stage the time saving offered by the present approach, relative to a full QM/MM PMF treatment. Here we start by the observation that the EVB umbrella-sampling procedure, which is comparable in terms of the time steps needed to standard PMF approaches, requires at least 30 windows with around 10000 configurations in each (assuming 10-ps long simulations with the usual 1-fs time step). Because each QM/MM step costs (e.g., in our case with B3LYP/6-31G\*) around 2 min on one 64-bit Intel Xeon 3.2 GHz processor, we would need 10<sup>4</sup> hours for an ab initio PMF calculation. This can be compared to a total of about 100 hours (involving 5000 single point calculations) that are required in our LRA approach that samples only the reactant, product, and the transition state (in contrast to a sampling along the entire reaction path). Of course, our approach can also benefit greatly from the similarity between the EVB and ab initio surface. Thus, by requiring that the EVB potential will be similar to the corresponding ab initial we can reduce the simulation length required for convergence.

Despite the advance of the present QM(ai)/MM treatment, it still involves an extensive and complicated procedure. Thus, it is encouraging to see that the catalytic effect obtained by the EVB method is quite reliable. Thus, we believe that many issues that require extensive configurational averaging (e.g., the effect of mutations and the relationship between folding energy and catalysis) should still be explored using the EVB method. In our view, the QM/MM-FEP treatment should be particularly important in cases where the exact mechanism in the enzyme presents an open question and also as a tool for refining and calibrating EVB studies of mutational effects.

**Acknowledgment.** This work was supported by NIH grants GM24492 and 1U19CA105010. We are grateful to Dr. P. K. Sharma for contributing to the ab initio calculations. The computational work was supported by University of Southern California High Performance Computing and Communication Center (HPCC).

#### References and Notes

- (1) Warshel, A.; Levitt, M. *J. Mol. Biol.* **1976**, *103*, 227.
- (2) Shurki, A.; Warshel, A. *Adv. Protein Chem.* **2003**, *66*, 249.



- (3) Gao, J. *Acc. Chem. Res.* **1996**, 29, 298.  
(4) Bakowies, D.; Thiel, W. *J. Phys. Chem.* **1996**, 100, 10580.  
(5) Field, M. J.; Bash, P. A.; Karplus, M. *J. Comput. Chem.* **1990**, 11, 700.  
(6) Friesner, R.; Beachy, M. D. *Curr. Opin. Struct. Biol.* **1998**, 8, 257.  
(7) Monard, G.; Merz, K. M. *Acc. Chem. Res.* **1999**, 32, 904.  
(8) Garcia-Viloca, M.; Gonzalez-Lafont, A.; Lluch, J. M. *J. Am. Chem. Soc.* **2001**, 123, 709.  
(9) Martí, S.; Andrés, J.; Moliner, V.; Silla, E.; Tunon, I.; Bertran, J. *Theor. Chem. Acc.* **2001**, 105, 207.  
(10) Field, M. J. *Comput. Chem.* **2002**, 23, 48.  
(11) Cui, Q.; Elstner, M.; Kaxiras, E.; Frauenheim, T.; Karplus, M. *J. Phys. Chem. B* **2001**, 105, 569.  
(12) Warshel, A.; Sussman, F.; Hwang, J. K. *J. Mol. Biol.* **1988**, 201, 139.  
(13) Muller, R. P.; Warshel, A. *J. Phys. Chem.* **1995**, 99, 17516.  
(14) Strajbl, M.; Hong, G.; Warshel, A. *J. Phys. Chem. B* **2002**, 106, 13333.  
(15) Olsson, M. H. M.; Hong, G.; Warshel, A. *J. Am. Chem. Soc.* **2003**, 125, 5025.  
(16) Zhang, Y.; Liu, H.; Yang, W. *J. Chem. Phys.* **2000**, 112, 3483.  
(17) Rod, T. H.; Ryde, U. *Phys. Rev. Lett.* **2005**, 94, 138302.  
(18) Liu, W. B.; Wood, R. H.; Doren, D. J. *J. Phys. Chem. B* **2003**, 107, 9505.  
(19) Iftimie, R.; Salahub, D.; Schofield, J. *J. Chem. Phys.* **2003**, 119, 11285.  
(20) Crespo, A.; Marti, M. A.; Estrin, D. A.; Roitberg, A. E. *J. Am. Chem. Soc.* **2005**, 127, 6940.  
(21) Sakane, S.; Yezdimer, E. M.; Liu, W.; Barriocanal, J. A.; Doren, D. J.; Wood, R. H. *J. Chem. Phys.* **2000**, 113, 2583.  
(22) Pradipta, B. *J. Chem. Phys.* **2005**, 122, 091102.  
(23) Hu, H.; Yang, W. *J. Chem. Phys.* **2005**, 123, 041102.  
(24) Strajbl, M.; Florián, J.; Warshel, A. *J. Am. Chem. Soc.* **2000**, 122, 5354.  
(25) Klahn, M.; Braun-Sand, S.; Rosta, E.; Warshel, A. *J. Phys. Chem. B* **2005**, 109, 15645.  
(26) Bentzien, J.; Muller, R. P.; Florian, J.; Warshel, A. *J. Phys. Chem. B* **1998**, 102, 2293.  
(27) Warshel, A. *Computer Modeling of Chemical Reactions in Enzymes and Solutions*; John Wiley & Sons: New York, 1991.  
(28) Warshel, A.; Parson, W. W. *Q. Rev. Biophys.* **2001**, 34, 563.  
(29) Shurki, A.; Strajbl, M.; Villa, J.; Warshel, A. *J. Am. Chem. Soc.* **2002**, 124, 4097.  
(30) Villa, J.; Warshel, A. *J. Phys. Chem. B* **2001**, 105, 7887.  
(31) Olsson, M. H. M.; Warshel, A. *J. Am. Chem. Soc.* **2004**, 126, 15167.  
(32) Verschuere, K. H. G.; Franken, S. M.; Rozeboom, H. J.; Kalk, K. H.; Dijkstra, B. W. *J. Mol. Biol.* **1993**, 232, 856.  
(33) Paneth, P. *Acc. Chem. Res.* **2003**, 36, 120.  
(34) Kmunicek, J.; Luengo, S.; Gago, F.; Ortiz, A. R.; Wade, R. C.; Damborsky, J. *Biochemistry* **2001**, 40, 11288.  
(35) Bosma, T.; Pikkemaat, M. G.; Kingma, J.; Dijk, J.; Janssen, D. B. *Biochemistry* **2003**, 42, 8047.  
(36) Kmunicek, J.; Hynkova, K.; Jedlicka, T.; Nagata, Y.; Negri, A.; Gago, F.; Wade, R. C.; Damborsky, J. *Biochemistry* **2005**, 44, 3390.  
(37) Soriano, A.; Silla, E.; Tunon, I.; Ruiz-Lopez, M. F. *J. Am. Chem. Soc.* **2005**, 127, 1946.  
(38) Bruice, T. C. *Acc. Chem. Res.* **2002**, 35, 139.  
(39) Lewandowicz, A.; Rudzinski, J.; Tronstad, L.; Widersten, M.; Ryberg, P.; Matsson, O.; Paneth, P. *J. Am. Chem. Soc.* **2001**, 123, 4550.  
(40) Marti, S.; Moliner, V.; Tunon, I. *J. Chem. Theory Comput.* **2005**, 1, 1008.  
(41) Bohac, M.; Nagata, Y.; Prokop, Z.; Prokop, M.; Monincova, M.; Tsuda, M.; Koca, J.; Damborsky, J. *Biochemistry* **2002**, 41, 14272.  
(42) Sun, H.; Kalju, K.; Thomas, B. *Proc. Natl. Acad. Sci. U.S.A.* **2003**, 100, 2215.  
(43) Pries, F.; Kingma, J.; Krooshof, G.; Jeronimus-Stratingh, C.; Bruins, A.; Janssen, D. *J. Biol. Chem.* **1995**, 270, 10405.  
(44) Nam, K.; Prat-Resina, X.; Garcia-Viloca, M.; Devi-Kesavan, L. S.; Gao, J. *J. Am. Chem. Soc.* **2004**, 126, 1369.  
(45) Devi-Kesavan, L. S.; Gao, J. *J. Am. Chem. Soc.* **2003**, 125, 1532.  
(46) Lau, E. Y.; Kahn, K.; Bash, P. A.; Bruice, T. C. *Proc. Natl. Acad. Sci. U.S.A.* **2000**, 97, 9937.  
(47) Devi-Kesavan, L. S.; Garcia-Viloca, M.; Gao, J. *Theor. Chim. Acta* **2003**, 109, 133.  
(48) Shaik, S. S.; Schlegel, H. B.; Wolfe, S. *Theoretical Aspects of Physical Organic Chemistry. Application to the SN2 Transition State*; Wiley-Interscience: New York, 1992.  
(49) Assfeld, X.; Rivail, J. *Chem Phys. Lett.* **1996**, 263, 100.  
(50) Chu, Z. T.; Villa, J.; Strajbl, M.; Schutz, C. N.; Shurki, A.; Warshel, A. *MOLARIS*, version beta9.05; University of Southern California, Los Angeles, CA, 2004.  
(51) Frisch, M. J.; Trucks, G. W.; Schlegel, H. B.; Scuseria, G. E.; Robb, M. A.; Cheeseman, J. R.; Zakrzewski, V. G.; Montgomery, J. A., Jr.; Stratmann, R. E.; Burant, J. C.; Dapprich, S.; Millam, J. M.; Daniels, A. D.; Kudin, K. N.; Strain, M. C.; Farkas, O.; Tomasi, J.; Barone, V.; Cossi, M.; Cammi, R.; Mennucci, B.; Pomelli, C.; Adamo, C.; Clifford, S.; Ochterski, J.; Petersson, G. A.; Ayala, P. Y.; Cui, Q.; Morokuma, K.; Malick, D. K.; Rabuck, A. D.; Raghavachari, K.; Foresman, J. B.; Cioslowski, J.; Ortiz, J. V.; Stefanov, B. B.; Liu, G.; Liashenko, A.; Piskorz, P.; Komaromi, I.; Gomperts, R.; Martin, R. L.; Fox, D. J.; Keith, T.; Al-Laham, M. A.; Peng, C. Y.; Nanayakkara, A.; Gonzalez, C.; Challacombe, M.; Gill, P. M. W.; Johnson, B. G.; Chen, W.; Wong, M. W.; Andres, J. L.; Head-Gordon, M.; Replogle, E. S.; Pople, J. A. *Gaussian 98*, revision A.9; Gaussian, Inc.: Pittsburgh, PA, 1998.  
(52) Maulitz, A. H.; Lightstone, F. C.; Zheng, Y.-J.; Bruice, T. C. *Proc. Natl. Acad. Sci. U.S.A.* **1997**, 94, 6591.  
(53) Florián, J.; Warshel, A. *J. Phys. Chem. B* **1997**, 101, 5583.